

Knowledge-Driven Federated Graph Learning on Model Heterogeneity

Zhengyu Wu, Guang Zeng, Huilin Lai, Daohan Su, Jishuo Jia, Yinlin Zhu, Xunkai Li, Rong-Hua Li, Guoren Wang, Chenghu Zhou

Abstract

Federated graph learning (FGL) has emerged as a promising paradigm for collaborative graph representation learning, enabling multiple parties to jointly train models while preserving data privacy. However, most existing approaches assume homogeneous client models and largely overlook the challenge of model-centric heterogeneous FGL (MHtFGL), which frequently arises in practice when organizations employ graph neural networks (GNNs) of different scales and architectures. Such architectural diversity not only undermines smooth server-side aggregation, which presupposes a unified representation space shared across clients' updates, but also further complicates the transfer and integration of structural knowledge across clients. To address this issue, we propose the Federated Graph Knowledge Collaboration (FedGKC) framework. FedGKC introduces a lightweight **Copilot Model** on each client to facilitate knowledge exchange while local architectures are heterogeneous across clients, and employs two complementary mechanisms: **Client-side Self-Mutual Knowledge Distillation**, which transfers effective knowledge between local and copilot models through bidirectional distillation with multi-view perturbation; and **Server-side Knowledge-Aware Model Aggregation**, which dynamically assigns aggregation weights based on knowledge provided by clients. Extensive experiments on eight benchmark datasets demonstrate that FedGKC achieves an average accuracy gain of 3.88% over baselines in MHtFGL scenarios, while maintaining excellent performance in homogeneous settings.

CCS Concepts

• **Computing methodologies** → **Semi-supervised learning settings**; **Neural networks**.

Keywords

Federated Graph Learning; Heterogeneity; Knowledge Distillation

ACM Reference Format:

Zhengyu Wu, Guang Zeng, Huilin Lai, Daohan Su, Jishuo Jia, Yinlin Zhu, Xunkai Li, Rong-Hua Li, Guoren Wang, Chenghu Zhou . 2026. Knowledge-Driven Federated Graph Learning on Model Heterogeneity. In . ACM, New York, NY, USA, 13 pages. <https://doi.org/10.1145/nnnnnnn.nnnnnnn>

Permission to make digital or hard copies of all or part of this work for personal or classroom use is granted without fee provided that copies are not made or distributed for profit or commercial advantage and that copies bear this notice and the full citation on the first page. Copyrights for components of this work owned by others than the author(s) must be honored. Abstracting with credit is permitted. To copy otherwise, or republish, to post on servers or to redistribute to lists, requires prior specific permission and/or a fee. Request permissions from permissions@acm.org.
Conference'17, July 2017, Washington, DC, USA

© 2026 Copyright held by the owner/author(s). Publication rights licensed to ACM.
ACM ISBN 978-x-xxxx-xxxx-x/YY/MM
<https://doi.org/10.1145/nnnnnnn.nnnnnnn>

1 Introduction

In today's data-driven world, graphs have become indispensable for representing complex relationships in domains such as social networks [16], bioinformatics [55], and recommendations [9]. Graphs effectively capture relational attributes and provide rich insights for machine learning. Graph Neural Networks (GNNs) [37] extend deep learning to non-Euclidean domains through message-passing mechanisms, enabling robust modeling that integrates local node features with global structural information. However, the rising data volume and privacy concerns expose the limitations of centralized training, which risks data leakage and hinders cross-entity collaboration. FGL [21] addresses these issues by training models locally and sharing only model updates, thus enabling collaborative learning while guaranteeing privacy and communication efficiency.

As FGL applications expand [23], the disparity between clients in data volume, computational resources, and data quality becomes non-negligible. Larger enterprises typically possess abundant data, allowing them to deploy large-scale GNNs [14, 40, 48]. In contrast, smaller companies with limited data may adopt lightweight or domain-specific models tailored to their unique operational contexts [32]. Existing research in FGL has primarily addressed data-centric heterogeneity [12, 17], while paying limited attention to the more fundamental **model-centric heterogeneity challenge** (MHtFGL), where divergent model architectures across clients introduce incompatibilities in representation learning and hinder effective knowledge integration at the server. Most FGL studies presuppose the homogeneous model architecture across clients, which curtails their applicability in practice. To bridge this gap, we propose a novel FGL framework designed to tackle the MHtFGL challenge while enhancing performance of collaborative training.

From a model-centric perspective, the essence of FGL lies in the client-server paradigm, wherein locally learned implicit knowledge must be effectively communicated between clients and the server to facilitate collaborative learning. The key to effective collaboration under MHtFGL lies in the choice of a proxy **Knowledge Carrier**, an alternative medium that replaces the shared model parameters [19, 46], which have long served as the default knowledge carrier but require an identical local model architecture for parameter alignment and convergence. Prior works have proposed alternative knowledge carriers, which can be boardly summarized into three categories: **(1) Prototype** [30, 47, 51]: They condense locally learned node representations into class-wise prototype vectors, which are typically low-dimensional embeddings summarizing local semantics. **(2) Public/Synthetic Information** [4, 42, 54]: The server stores either the Public dataset or collaboratively trained synthetic Generators, which are utilized as the reference medium. They are distributed to local clients, who then align their local training using knowledge carriers such as prediction logits, gradients, or generator parameters, etc. **(3) Partial Model** [1, 24, 36]: The

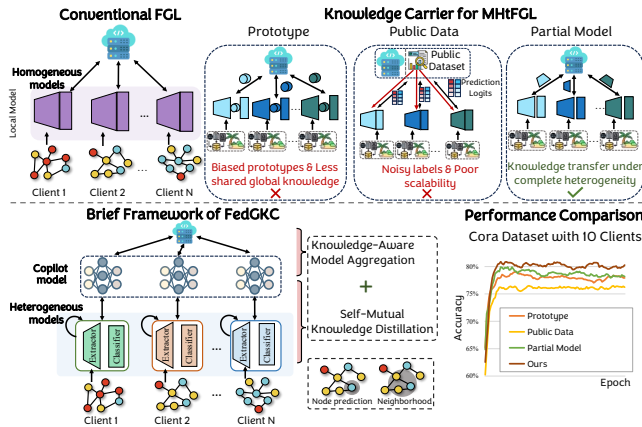


Figure 1: Illustration of the conventional FGL, heterogeneous federated learning approaches, and our proposed FedGKC.

server either distributes a homogeneous model component shared across heterogeneous clients or allocates model subsets of varying depth or parameter scale according to each client’s computational capacity and the relevance of parameter subsets to its local data distribution. Within the context of FGL, **Partial Model** can be regarded as the most effective solution since the strength of GNNs stems from the neighbor aggregation and propagation mechanism, through which implicit graph knowledge is tightly entangled with the trained model parameters themselves. In contrast, the knowledge carriers employed by the other two strategies rely primarily on model outputs (e.g., logits or gradients), which can only serve as indirect reflections of the underlying graph-structural knowledge.

Although effective, existing Partial Model strategies face notable limitations. Sharing activations or aligned model layers poses privacy risks and limits scalability as client numbers and diversity of local model architectures increase. The exchanged submodels are typically topology-agnostic components (e.g., classification heads), whose aggregation yields suboptimal performance since graph knowledge is inherently topology-dependent. To overcome these issues, we introduce a lightweight **Copilot Model** (illustrated in Fig. 1) as a dedicated, architecture-agnostic knowledge carrier for cross-client transfer. It acts as an auxiliary module trained via knowledge distillation coupled with topology-aware objectives, enabling it to capture both feature semantics and structural dependencies from the local training. As shown in Fig. 1, a toy experiment on the 10-client Cora dataset demonstrates that while Partial Model outperform other paradigms, our approach, as an innovative paradigm to Partial Model, achieves the best efficiency and effectiveness. Implementation details are provided in Appendix C.1.

Building on the above analysis, we propose the **Federated Graph Knowledge Collaboration (FedGKC)** framework to address MHt-FGL. The framework leverages knowledge distillation while explicitly adapting it to structural properties of graph data. To this end, we introduce copilot models on the client-side to bridge architectural differences and design a knowledge-aware aggregation strategy on the server-side to ensure effective integration of diverse knowledge uploaded from clients. Specifically, FedGKC consists

of two key components: **(1) Self-Mutual Knowledge Distillation (SMKD)** on heterogeneous clients. We establish a bidirectional knowledge distillation process between each local model and its copilot model. This design enables the copilot to acquire localized knowledge while simultaneously injecting global knowledge back into the local model. Beyond class-level predictions, SMKD also transfers neighborhood information, thereby enhancing the model’s ability to capture topological dependencies. (Sec. 3.3.1) To improve robustness, we incorporate a multi-view data perturbation strategy for local self-distillation, ensuring consistent predictions across perturbed local graphs, and boosting generalizabilities. (Sec. 3.3.2) **(2) Knowledge-Aware Model Aggregation (KAMA)** on the server side. Unlike the conventional FedAvg algorithm [26], which assigns weights to clients solely based on their data volume, KAMA recognizes that heterogeneous clients differ significantly in learning capacity and knowledge quality. Specifically, we design an adaptive weighting mechanism based on data volume, knowledge strength, and knowledge clarity. Performing aggregation on knowledge-aware weights, KAMA achieves more accurate and efficient integration between clients, guiding the global model toward better convergence.

To summarize, our work offers three following contributions: **(1) Problem Identification.** We are the first to systematically investigate the challenge of MHtFGL, specifically the partial model strategy, where diverse client architectures hinder unified training and complicate the integration of graph knowledge in real-world deployments. **(2) Innovative Framework.** We propose **FedGKC**, a knowledge-driven FGL framework that enables effective collaboration across clients with heterogeneous models. It incorporates two key mechanisms: SMKD, which bridges structural differences through bidirectional and topology-aware knowledge distillation between local and copilot models; and KAMA, which adaptively aggregates client contributions based on knowledge quality, ensuring more reliable global insights. **(3) Superior Performance.** We validate FedGKC on eight benchmark datasets under both heterogeneous and homogeneous settings. Experiments show consistent improvements, with an average accuracy gain of 3.88% and up to 8.13% over state-of-the-art baselines, confirming both the effectiveness and generalizability of our approach.

2 Related Works

2.1 Federated Graph Learning

FGL extends FL to GNNs and enables collaborative training on graph-structured data while preserving data privacy. Instead of exchanging raw data, clients upload learned graph representation models to the secured server to aggregate cross-client knowledge. Existing FGL research can be broadly categorized into two settings: **(1) Graph-FL:** Each client owns multiple independent graphs and the goal is to address graph-level tasks (e.g., graph classification). Representative approaches include GCFL [38] and FedStar [29], etc. **(2) Subgraph-FL:** Each client holds a subgraph of an implicit global graph and the objective is to solve node-level tasks (e.g., node classification). Representative works include FGSSL [12], FedGTA [17], FedPub [2], and FedSage+ [52]. Notably, previous studies have concentrated on addressing data heterogeneity challenges [12, 17]. However, in real-world scenarios, GNNs from different clients may

deploy divergent architectural models, posing fundamental obstacles to unified graph learning and complicating collaborative training. To the best of our knowledge, we are the first to investigate this issue and propose the new paradigm tailored for this challenge.

2.2 Model-Centric Heterogeneous FL

Model-centric heterogeneous federated learning (MHtFL) enables flexible and diverse client architectures while preserving data privacy. Existing MHtFL methods can be broadly classified into three categories, each with distinct limitations: **(1) Prototype** [30, 31, 51] avoid sharing parameters but suffer from biased classifiers, further exacerbated by architectural diversity [18], which undermines efficacy of the global knowledge aggregation. **(2) Public/Synthetic Information** [4, 20, 42, 50, 54] distribute globally stored public dataset or generators for synthesizing graph information to clients. During local training, heterogeneous clients align their predictions or gradients on shared public data or upload generator parameters for aggregation. However, such proxies act as indirect knowledge carriers and fail to capture the topology-dependent structural knowledge that is crucial for effective FGL training. **(3) Partial Model** methods such as LG-FedAvg [19], FedGen [57], and FedGH [46] permit heterogeneity in major model components while enforcing homogeneity on a small shared module. This design enables limited global knowledge transfer but constrains model expressiveness. Approaches such as FML [28] and FedKD [34] employ auxiliary global models for mutual distillation; however, early training rounds risk exchanging low-quality or unstable knowledge.

Notably, these approaches are not specifically tailored for graph-structured data. To address the issue, we propose an approach that employs knowledge distillation to facilitate effective graph information transfer between local heterogeneous models and a globally shared Copilot Model during local training, thereby balancing personalized local knowledge and global generalizability.

2.3 Knowledge Distillation on Graph

Knowledge distillation (KD) [10] transfers knowledge from large models to smaller ones, reducing computational cost while preserving performance. In graph learning, KD enables knowledge transfer across diverse models, with the main challenge being what knowledge to distill and how to distill it.

Three main categories of transferable knowledge are commonly explored: **(1) Logits**, i.e., outputs before the Softmax layer, where methods minimize distribution divergence to transfer predictive knowledge [33, 41, 43]. **(2) Graph structure**, which captures node-edge connectivity and relationships, with approaches aligning nodes via neighborhood relations to transfer structural information [6, 44]. **(3) Embeddings**, i.e., intermediate node representations extracted from hidden layers, which contain feature and structural context. It can be distilled to guide another model's training [8, 13, 49].

Regarding distillation methods, direct distillation minimizes differences between models, promoting intuitive knowledge transfer [41]; adaptive distillation offers flexibility by considering the importance of different knowledge components. Methods like RDD [53], FreeKD [5], and MulDE [33] adjust the distillation process based on the certainty or correctness of the knowledge, allowing models to focus more on reliable information while avoiding knowledge that

is less informative or noisy. Furthermore, various distillation strategies tailored for specific tasks exist within machine learning [8]. Our study aims to ensure the preservation and transfer of effective graph information within heterogeneous federated scenarios, thereby facilitating collaborative training among multiple clients.

3 Methodology

3.1 Notations and Problem Formulation

In this study, we propose an MHtFGL framework designed to leverage diverse graph data and GNN models from multiple clients for collaborative training, while ensuring the protection of data privacy.

Let there be K clients, where the graph data owned by client k is represented as $G_k = (V_k, E_k)$ with $|V_k| = N_k$ nodes and $|E_k| = M_k$ edges. The graph's adjacency matrix, node feature matrix, and label matrix are denoted as $A_k \in \mathbb{R}^{N_k \times N_k}$, $X_k \in \mathbb{R}^{N_k \times f}$, and $Y_k \in \mathbb{R}^{N_k \times C}$, respectively, where f represents the number of node features and C denotes the number of classes. Note that the graph data and the GNN model architectures can vary among different clients.

GNNs constitute a class of deep learning models tailored to perform embedding and inference tasks on graph-structured data. Federated learning is a collaborative learning paradigm that enables the training of a shared model across multiple data owners without the direct exchange of raw data. Each training round involves the selection of participating clients, the update of the local model via local training on each chosen client, the aggregation of local model parameters on a central server, and the subsequent distribution of the aggregated parameters back to the clients. The objective of our work is to enhance the performance of each client's local model on node classification tasks in heterogeneous environments.

3.2 Overview

In this section, we properly present our proposed FedGKC, whose overall training architecture is illustrated in Fig. 2. At first, the parameters of all models are initialized. Then, the following steps are executed in each round of federated training: (1) Local model and its received copilot model on each client are trained following objectives defined in Self-Mutual Knowledge Distillation (SMKD). (2) At the server, FedGKC performs Knowledge-Aware Model Aggregation (KAMA) with uploaded messages indicating local knowledge strength and clarity alongside updated copilot model parameters from each client. (3) The aggregated model parameters are distributed back to all client copilot models. Steps (1) to (3) are repeated until convergence, allowing each client's local model to learn global knowledge without transmitting graph data, guaranteeing on aligning the local and global optimizing direction.

3.3 Self-Mutual Knowledge Distillation

The model learning process on the client side consists of two main components. Firstly, there is a mutual knowledge learning process between the local model and the copilot model. This process not only allows the copilot model to acquire more localized knowledge but also enables the local model to obtain global knowledge that includes information from other clients. Secondly, to enhance the predictive capability of the local model, we generate two different views by perturbing graph elements from the same graph to

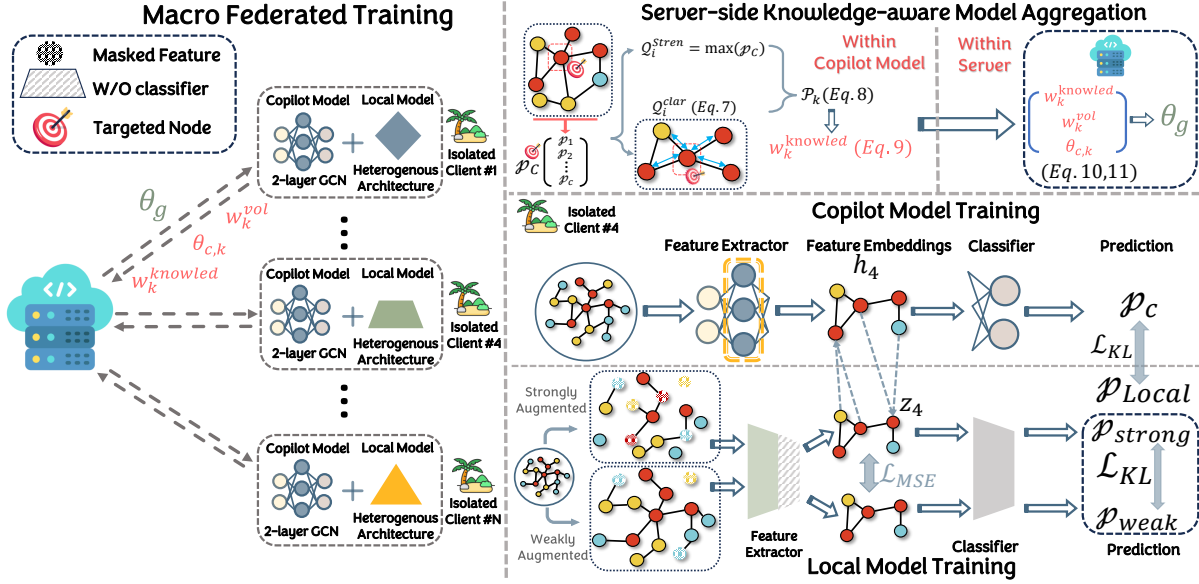


Figure 2: The visualized training pipeline of FedGKC. The Macro Federated Training depicts the FGL architecture in its essence, in which each client uploads its data volume: w_k^{vol} , trained copilot model parameters: $\theta_{c,k}$, and knowledge-realized weights: $w_k^{knowled}$, to secured server for model aggregation. On clients, heterogenous model architectures are implemented, which are visually separated by different shapes and colors. The right-hand side of the figure use the Isolated Client #4 showcases the training. Notably, to have a better visual illustration for readers, we use fewer nodes from the same subgraph dataset to increase its display clarity. All symbols in the figure are aligned with our methodological descriptions in Sec. 3.2. Copilot Model Training and Local Model Training refer to Sec. 3.3.1, and Server-side Knowledge-aware Model Aggregation refers to Sec. 3.4.

implement self-distillation. This ensures that local model generates consistent and robust embeddings and predictions.

3.3.1 Mutual distillation addressing model heterogeneity. In traditional knowledge distillation methods [43], knowledge is typically transferred by aligning the prediction results of different models on the same data. However, merely aligning the prediction results may limit the knowledge learned by the models, resulting in a lack of comprehensiveness and representativeness. In the context of graph data processed by GNNs, node representations are primarily derived from capturing neighborhood information. Therefore, we propose propagating neighborhood knowledge to enhance the utilization of topological information captured by GNNs:

$$\mathcal{L}_{\text{neigh}} = \frac{1}{|N|} \sum_{i \in N} \sum_{j \in \mathcal{V}_i \cup i} \mathcal{D}(\sigma(z_j), \sigma(h_i)), \quad (1)$$

where z and h represent the embedding outputs of the feature extractor of the two models, respectively. \mathcal{V}_i represents the set of neighbor nodes of node i , N denotes the total number of nodes, $\sigma = \text{softmax}(\cdot)$ denotes an activation function, and $\mathcal{D}(\cdot)$ denotes a distance function (e.g., Kullback Leibler divergence [10]).

For the copilot model, the optimization objective is denoted as:

$$\mathcal{L}_{\text{cop-mutu}} = \alpha \mathcal{L}_{CE}(y, p_c) + \beta \mathcal{L}_{\text{neigh}} + (1 - \alpha - \beta) \mathcal{L}_{KL}(p_l \| p_c), \quad (2)$$

where α and β are the weights to balance the influence of different distillation losses, and p_l and p_c are the predictions of local and copilot models, respectively. Here, \mathcal{L}_{KL} is the KL divergence function, and $\mathcal{L}_{CE}(y, p_c) = -y \log(\text{softmax}(p_c))$ represents the cross-entropy loss between p_c and the truth label y .

Similarly, the local model learn information from the copilot model and train on local data, and its optimization objective is:

$$\mathcal{L}_{\text{local-mutu}} = \alpha \mathcal{L}_{CE}(y, p_l) + \beta \mathcal{L}_{\text{neigh}} + (1 - \alpha - \beta) \mathcal{L}_{KL}(p_c \| p_l). \quad (3)$$

3.3.2 Self-distillation mining model potential. To further stimulate the performance of the local model, we introduce a self-distillation strategy. We first create two perspectives on the same graph data, a strongly perturbed view and a weakly perturbed view. This dual-perspective strategy effectively enhances the diversity of graph data by applying varying degrees of edge removal and feature masking [56]. The weakly perturbed view retains more original information, while the strongly perturbed view significantly obscures and removes more graph information (e.g., topological structure, node semantics). We expect the predictions of the strongly perturbed view to closely align with the predictions of the weakly perturbed view for the same input. It aims to ensure that, even when faced with substantial information alteration, the local model maintains consistency in its predictions, thereby deepening its understanding of the data's intrinsic nature. The optimization objective for the self-distillation of the local model is denoted as

$$\mathcal{L}_{\text{self-distill}} = \mathcal{L}_{MSE}(e_l^{\text{weak}}, e_l^{\text{strong}}) + \mathcal{L}_{KL}(p_l^{\text{weak}} \| p_l^{\text{strong}}), \quad (4)$$

where \mathcal{L}_{MSE} denotes the mean-square error loss, and e and p represent the embedding outputs of the model feature extractor and the prediction outputs of the classifier, respectively. In summary, the overall optimization objective for the local model integrates the mutual distillation objective with the self-distillation objective:

$$\mathcal{L}_{\text{local}} = \mathcal{L}_{\text{local-mutu}} + \mathcal{L}_{\text{self-distill}}. \quad (5)$$

The optimization goal for the copilot model is shown in Eq. (2). This coordinated optimization enhances the learning efficiency and knowledge acquisition capability of the local model in MHFGL.

3.4 Knowledge-Aware Model Aggregation

Given the heterogeneity among clients, the learning efficiency of each client's model varies accordingly. Traditional FL methods typically employ an averaging aggregation strategy [26], which does not take into account the model heterogeneity scenario. This oversight results in conflicted models aggregation and suboptimal overall performance. To address it, we propose a Knowledge-Aware Model Aggregation mechanism that dynamically assigns weights based on learned knowledge quality of each client's model. Through dynamic weighting, well-informed clients is protected from the adverse effects of clients with limited knowledge. Simultaneously, it channels greater guidance from knowledgeable clients to less-informed ones, improving convergence and robustness.

Specifically, when aggregating the copilot models from each client, the server first considers the **data volume** from an overall perspective and calculates volume weight accordingly, denoted as:

$$w_k^{vol} = \frac{N_k}{\sum_{k=1}^K N_k}, \quad (6)$$

where N_k indicates the amount of data on the k -th client.

Next, it assesses the knowledge levels learned by each node in the copilot model. Ideally, each node should focus on relevant knowledge associated with its respective category, implying that the knowledge should be strong and clear. We measure knowledge level from two dimensions: **knowledge strength** and **knowledge clarity**. The knowledge strength at a node can be represented by the maximum value of the output prediction probabilities, which intuitively reflects the model's confidence in recognizing a particular category, denoted as $Q_i^{stren} = \max(p_i)$. On the other hand, assessing knowledge clarity is more complex as it involves evaluating the distinction between the predictions of this node and those of other categories, expressed as $Q_i^{stren} - \sum p_i^*$, where p^* represents the set of values other than the maximum value. Additionally, we must be wary of the over-smoothing phenomenon in GNNs due to interactions with neighbor nodes, which compromises the model's discriminatory ability. The clarity evaluation is formulated as:

$$Q_i^{clar} = \frac{1}{M-1} \left(Q_i^{stren} - \sum p_i^* \right) - \lambda \left(\frac{1}{|\mathcal{V}_i|} \sum_{j \in \mathcal{V}_i} \text{sim}(p_i, p_j) \right), \quad (7)$$

where M represents the number of categories, \mathcal{V}_i represents the set of neighbor nodes of node i , λ is the weight of the over-smoothing effect, and $\text{sim}(\cdot)$ represents the cosine similarity calculation. Then, the degree of knowledge mastery of each client is quantified by:

$$\mathcal{P}_k = \frac{1}{N_k} \sum_{i=1}^{N_k} \left(Q_i^{stren} + Q_i^{clar} \right), \quad (8)$$

where N_k indicates the amount of data on the k -th client. The knowledge-related weights are expressed as:

$$w_k^{knowled} = \frac{\mathcal{P}_k}{\sum_{k=1}^K \mathcal{P}_k}. \quad (9)$$

Algorithm 1 The complete algorithm of FedGKC

Input: Communication round T ; Initial model parameters θ ; The number of clients K ;
Output: Local models for all clients;
1: Initialize all client-side copilot and local models;
2: **for** $t = 1, \dots, T$ **do**
3: // **Client Side:**
4: **for** $k = 1, \dots, K$ in parallel **do**
5: Optimize the copilot model according to Eq. (2);
6: Optimize the local model according to Eq. (5);
7: Record the data volume N_k ;
8: Calculate the knowledge level \mathcal{P}_k through Eq. (8);
9: **end for**
10: // **Server Side:**
11: Compute the model aggregation weights w_k by Eq. (10);
12: Update aggregate model parameters by Eq. (11);
13: Send aggregate model parameters to the client-side copilot model: $\theta_{c,k} \leftarrow \theta_g$;
14: **end for**

By considering data volume, node knowledge strength, and node knowledge clarity, we quantify the learning knowledge level of each client's copilot model. Consequently, the aggregation weight for the k -th client's model can be determined as follows:

$$w_k = \left(w_k^{vol} + w_k^{knowled} \right) / 2. \quad (10)$$

The model aggregation formula is:

$$\theta_g = \sum_{k=1}^K w_k \cdot \theta_{c,k}, \quad (11)$$

where $\theta_{c,k}$ is the parameters of the k -th client copilot model.

Finally, the aggregated model parameters will be distributed back to each client's copilot model in preparation for the next round of client training. Through this meticulous adjustment, our aggregation strategy effectively integrates multi-source information, achieving a more efficient and equitable model aggregation process. The complete algorithm of FedGKC is presented in Algorithm 1.

3.5 Complexity Analysis

We now provide a computational complexity analysis of FedGKC. Each client employs a GNN as the local model. For an l -layer GNN model with a batch size b , the propagated feature $X^{(l)}$ has a space complexity of $O((b+l)f)$, and the overhead for linear regression operations is $O(f^2)$, where f are the number of feature dimensions. The introduction of the copilot model doubles the parameter storage space, leading to an overall space complexity of $O(2(b+l)f + 2f^2)$. Furthermore, the inclusion of additional alignment losses within the self-mutual knowledge distillation module introduces a time complexity of $O(f^2)$. For the server, the reception and aggregation of model parameters impose space and time complexities of $O(Nf^2)$ and $O(N)$, respectively, where N represents the number of clients involved. Therefore, the total space complexity is dominated by client-side storage and server-side aggregation, yielding $O(2N(b+l)f + 2Nf^2)$. The total time complexity per communication round is primarily governed by client-side local training

and server-weighted aggregation, resulting in $O(N(b+l)f + Nf^2)$. Compared to conventional FGL methods, FedGKC introduces manageable overhead through its knowledge distillation and knowledge-aware aggregation mechanisms, achieving an effective balance between efficiency and performance. The detailed analysis and comparison can be found in Appendix A.

4 Theoretical Analysis

To substantiate the effectiveness of FedGKC and improve its theoretical interpretability, we show that SMKD enhances stability and robustness, while KAMA drives the descent direction closer to the global optimum compared to conventional federated learning.

4.1 Stability and Robustness of SMKD

To rigorously characterize the stability of embeddings under perturbation, we introduce a finite difference Lipschitz constant. In conjunction with the definition of our self-distillation loss and its associated inequality relations, we have Definition 1 and Theorem 1.

DEFINITION 1 (LIPSCHITZ CONSTANT). *For each sample i , we define the perturbation gap between strong and weak views as Δ_i and according to the perturbation gap, we define the finite difference Lipschitz constant of embeddings as:*

$$\Delta_i := x_i^{\text{strong}} - x_i^{\text{weak}}, \quad \hat{L}_e(i) := \frac{\|e(x_i^{\text{strong}}) - e(x_i^{\text{weak}})\|}{\|\Delta_i\|}. \quad (12)$$

THEOREM 1. *The squared discrepancy between the strong and weak perturbations, measured by the normalized embedding difference, is upper bounded by the ratio of the self-distillation loss to the average squared perturbation magnitude.*

$$\frac{1}{N} \sum_{i=1}^N \hat{L}_e(i)^2 \leq \frac{L_{\text{self}}}{\frac{1}{N} \sum_{i=1}^N \|\Delta_i\|^2}. \quad (13)$$

As training progresses, L_{self} gradually decreases, leading to a corresponding reduction of the Lipschitz constant. Consequently, it demonstrates that the embeddings become insensitive to perturbations in the input data.

4.2 Gradient Direction in KAMA

We first define the local descent direction of the k -th client as g_k , the ideal optimal descent direction as g^* , and the alignment measure as $a_k = \langle g_k, g^* \rangle$. According to the definition of knowledge clarity and our formulation of the aggregation weights, we obtain Theorem 2.

THEOREM 2. *The node score S_i is defined as the sum of knowledge strength and knowledge clarity, where $\overline{\text{sim}}_i$ represents the mean similarity among neighboring nodes of node i .*

$$S_i := Q_i^{\text{stren}} + Q_i^{\text{clar}} = \left(1 + \frac{2}{M-1}\right) m_i - \frac{1}{M-1} - \lambda \overline{\text{sim}}_i. \quad (14)$$

Furthermore, it can be derived that the node score S_i exhibits monotonic growth with respect to the highest probability m_i and monotonic decline with respect to the average neighborhood similarity. Therefore, our aggregation weights effectively capture greater knowledge quality. The magnitude of the aggregation weight is positively correlated with the degree of alignment.

Based on our definition, the inner products of the two aggregated directions with g_i are given as follows:

$$\langle \hat{g}_{\text{FedAvg}}, g^* \rangle = \sum_k w_k^{\text{vol}} a_k, \quad \langle \hat{g}_{\text{KAMA}}, g^* \rangle = \sum_k w_k a_k. \quad (15)$$

Thus, we have our Theorem 3.

THEOREM 3. *The difference between the inner products of the two aggregated directions can be derived as the following expression, where \bar{P} and \bar{a} denote the average aggregation weight and alignment across clients, respectively.*

$$\langle \hat{g}_{\text{KAMA}}, g^* \rangle - \langle \hat{g}_{\text{FedAvg}}, g^* \rangle = \frac{1}{2} \left(\bar{a} - \sum_k w_k^{\text{vol}} a_k + \frac{\text{Cov}(P, a)}{\bar{P}} \right). \quad (16)$$

Under the unbiased sampling condition, the first term on the right-hand side can be regarded as zero. Moreover, by Theorem 2, $\text{Cov}(P, a)$ is positive. Consequently, it demonstrates that the KAMA module ensures the descent direction of optimization is closer to the global optimum compared to conventional FL approaches such as FedAvg. Detailed proofs of Theorems are in the Appendix B.

5 Experiments

In this section, a comprehensive evaluation of FedGKC is provided. We aim to answer following key questions: **Q1:** Does FedGKC exhibit superior performance compared to state-of-the-art baseline methods? **Q2:** What contributes to the performance enhancement of FedGKC? **Q3:** Is FedGKC capable of generalizing effectively across varying copilot model architectures? **Q4:** How resilient is the performance of FedGKC to fluctuations in hyperparameter values?

5.1 Experimental Setup

5.1.1 Datasets. Experiments are conducted utilizing 8 commonly employed benchmark datasets in graph learning. These consist of three small-scale citation networks (Cora, CiteSeer, PubMed) [45], two medium-scale co-authorship networks (CS, Physics) [27], two medium-scale user-item datasets (Photo, Computer) [25], and one large-scale open graph benchmark dataset (ogbn-arxiv) [11]. Further particulars regarding these datasets are delineated in Table 6.

5.1.2 Baselines. We compare FedGKC with heterogeneous federation strategies. Given the absence of strategies for MHTFGL, we re-implemented these methods under FGL conditions based on the available source code. There are personalization-based strategies (e.g., LG-FedAvg [19]), prototype-based approaches (e.g., FedProto [30], FedTGP [51]), knowledge distillation-based methods (e.g., FML [28], FedKD [34]), partial-model based model FIARSE [36] and method for MHTFGL called FedPPN [22]. Due to the need for partial homogeneity of the personalization method, we set up the same classifier for all clients when implementing the LG-FedAvg. In addition, we maintain a completely heterogeneous framework for all client models. The detailed implementations are in Appendix C.

5.1.3 Heterogeneity Simulations. To partition data to each client, we deploy Louvain [3] community detection algorithm to partition graph into subgraphs that are distributed to clients. To ensure uniformity and simulate multi-clients scenarios, we conduct experiments using configurations of 5, 10, and 20 clients. Specifically, we consider two model heterogeneity scenarios: **(1) Divergent model**

Table 1: Performance comparison in Divergent Model Architectures. The best and sub-best results are marked in Red and Blue.

Method	Cora			CiteSeer			PubMed			ogbn-arxiv		
	5	10	20	5	10	20	5	10	20	5	10	20
LG-FedAvg	78.78 \pm 0.33	78.11 \pm 0.12	70.52 \pm 0.58	65.64 \pm 0.47	62.74 \pm 0.29	58.57 \pm 0.64	84.52 \pm 0.36	82.74 \pm 0.52	80.95 \pm 0.27	61.32 \pm 0.41	61.29 \pm 0.38	61.62 \pm 0.49
FedProto	78.50 \pm 0.77	77.75 \pm 0.22	74.13 \pm 0.27	59.77 \pm 1.17	59.26 \pm 0.77	57.28 \pm 0.81	84.71 \pm 0.25	82.77 \pm 0.04	81.74 \pm 0.13	38.26 \pm 2.13	44.82 \pm 1.92	48.19 \pm 0.73
FML	80.33 \pm 0.44	79.90 \pm 0.39	75.37 \pm 0.52	64.67 \pm 0.46	62.52 \pm 0.41	60.39 \pm 0.57	84.39 \pm 0.33	83.05 \pm 0.48	82.23 \pm 0.36	52.15 \pm 0.71	58.25 \pm 0.65	60.98 \pm 0.49
FedKD	80.32 \pm 1.07	78.64 \pm 0.43	73.01 \pm 0.75	65.19 \pm 0.64	62.22 \pm 0.57	59.58 \pm 1.00	85.37 \pm 0.09	83.21 \pm 0.16	82.19 \pm 0.17	51.77 \pm 2.22	61.31 \pm 0.25	63.34 \pm 0.19
FedTGP	79.50 \pm 1.40	78.47 \pm 0.64	74.58 \pm 0.35	61.10 \pm 0.72	59.47 \pm 0.77	59.30 \pm 0.48	85.01 \pm 0.20	83.36 \pm 0.13	81.34 \pm 0.13	42.08 \pm 1.93	49.43 \pm 2.00	54.24 \pm 0.45
FIARSE	77.96 \pm 0.30	78.91 \pm 0.28	73.96 \pm 0.40	65.17 \pm 0.96	63.43 \pm 0.46	60.45 \pm 0.68	85.38 \pm 0.22	83.24 \pm 0.11	82.32 \pm 0.14	60.10 \pm 0.32	61.45 \pm 0.26	61.49 \pm 0.10
FedPPN	76.69 \pm 0.52	78.46 \pm 0.36	74.94 \pm 0.27	64.87 \pm 0.72	63.00 \pm 0.51	60.26 \pm 0.36	85.33 \pm 0.19	82.44 \pm 0.19	82.01 \pm 0.10	60.14 \pm 0.22	61.89 \pm 0.12	62.75 \pm 0.25
TRUST	79.89 \pm 0.22	78.67 \pm 0.26	74.76 \pm 0.32	65.06 \pm 0.57	63.16 \pm 0.32	60.32 \pm 0.45	85.28 \pm 0.21	82.83 \pm 0.17	82.12 \pm 0.12	61.34 \pm 0.32	61.93 \pm 0.25	62.92 \pm 0.31
FedGKC	83.42 \pm 0.45	82.71 \pm 0.62	76.38 \pm 0.38	68.19 \pm 0.46	66.15 \pm 0.73	63.40 \pm 0.67	87.54 \pm 0.16	85.48 \pm 0.25	84.42 \pm 0.11	63.47 \pm 1.90	62.58 \pm 1.60	65.29 \pm 4.98

Method	CS			Physics			Photo			Computer		
	5	10	20	5	10	20	5	10	20	5	10	20
LG-FedAvg	88.07 \pm 0.44	87.16 \pm 0.31	82.69 \pm 0.57	94.26 \pm 0.28	91.79 \pm 0.35	92.24 \pm 0.46	90.41 \pm 0.53	86.81 \pm 0.40	85.11 \pm 0.48	87.42 \pm 0.42	85.99 \pm 0.37	83.79 \pm 0.55
FedProto	84.09 \pm 0.38	83.49 \pm 0.46	81.24 \pm 0.24	92.87 \pm 0.11	92.54 \pm 0.11	91.81 \pm 0.10	71.93 \pm 0.06	75.38 \pm 1.52	79.37 \pm 1.22	57.61 \pm 2.55	75.55 \pm 2.04	71.35 \pm 0.74
FML	87.34 \pm 0.42	85.93 \pm 0.36	83.34 \pm 0.49	93.03 \pm 0.27	92.58 \pm 0.33	92.11 \pm 0.39	89.80 \pm 0.44	86.84 \pm 0.41	79.97 \pm 0.52	87.64 \pm 0.47	83.08 \pm 0.46	78.18 \pm 0.40
FedKD	88.47 \pm 0.15	86.46 \pm 0.31	83.43 \pm 0.28	93.21 \pm 0.36	92.81 \pm 0.20	91.86 \pm 0.12	89.90 \pm 0.32	84.96 \pm 1.18	86.74 \pm 0.58	78.53 \pm 4.60	83.69 \pm 0.85	78.47 \pm 1.34
FedTGP	85.88 \pm 0.15	84.99 \pm 0.24	82.29 \pm 0.32	93.42 \pm 0.19	93.12 \pm 0.12	92.26 \pm 0.10	75.31 \pm 3.61	81.04 \pm 1.19	80.13 \pm 0.30	67.30 \pm 4.97	73.76 \pm 1.58	71.85 \pm 1.64
FIARSE	87.33 \pm 0.23	86.75 \pm 0.28	84.26 \pm 0.33	93.92 \pm 0.11	92.97 \pm 0.08	92.20 \pm 0.05	90.84 \pm 0.38	89.49 \pm 0.22	88.38 \pm 0.15	87.71 \pm 0.30	86.47 \pm 0.19	84.52 \pm 0.41
FedPPN	86.67 \pm 0.21	86.59 \pm 0.20	84.10 \pm 0.25	93.57 \pm 0.11	93.12 \pm 0.08	91.83 \pm 0.15	90.38 \pm 0.35	90.33 \pm 0.28	88.48 \pm 0.20	87.71 \pm 0.17	86.09 \pm 0.53	84.91 \pm 0.24
TRUST	87.53 \pm 0.32	85.78 \pm 0.24	83.32 \pm 0.31	94.43 \pm 0.22	92.56 \pm 0.15	92.05 \pm 0.21	89.45 \pm 0.24	82.44 \pm 0.19	89.45 \pm 0.18	84.32 \pm 0.15	83.57 \pm 0.25	82.94 \pm 0.32
FedGKC	89.62 \pm 0.15	88.31 \pm 0.27	86.04 \pm 0.14	95.71 \pm 0.27	94.75 \pm 0.15	93.56 \pm 0.26	93.19 \pm 0.67	91.65 \pm 0.32	89.76 \pm 0.43	88.57 \pm 0.34	87.90 \pm 0.32	86.84 \pm 0.32

Table 2: Performance comparison in Varying Model Scales. The best and sub-best results are marked in Red and Blue.

Method	Cora			CiteSeer			PubMed			ogbn-arxiv		
	5	10	20	5	10	20	5	10	20	5	10	20
LG-FedAvg	79.50 \pm 0.42	79.90 \pm 0.37	73.43 \pm 0.55	66.16 \pm 0.44	65.47 \pm 0.39	58.62 \pm 0.52	84.48 \pm 0.41	83.17 \pm 0.46	80.70 \pm 0.38	62.24 \pm 0.47	65.05 \pm 0.51	65.32 \pm 0.43
FedProto	77.59 \pm 0.61	78.19 \pm 0.57	72.55 \pm 0.21	62.08 \pm 0.91	57.70 \pm 1.47	57.03 \pm 0.33	84.71 \pm 3.32	83.08 \pm 0.30	81.27 \pm 0.27	50.06 \pm 1.34	53.92 \pm 0.91	57.04 \pm 0.25
FML	80.42 \pm 0.48	79.18 \pm 0.39	74.23 \pm 0.44	66.23 \pm 0.36	64.30 \pm 0.41	61.10 \pm 0.52	84.76 \pm 0.47	83.13 \pm 0.42	81.43 \pm 0.38	54.89 \pm 0.56	62.43 \pm 0.49	64.62 \pm 0.45
FedKD	80.23 \pm 0.47	79.81 \pm 0.56	74.13 \pm 0.39	66.46 \pm 0.94	65.92 \pm 1.26	60.30 \pm 0.58	85.08 \pm 2.51	83.25 \pm 0.16	82.21 \pm 0.66	59.71 \pm 0.87	61.06 \pm 6.22	63.68 \pm 5.00
FedTGP	78.23 \pm 0.75	78.65 \pm 0.66	73.25 \pm 0.44	63.12 \pm 0.61	58.60 \pm 0.73	58.55 \pm 0.65	84.43 \pm 2.95	83.32 \pm 0.16	81.12 \pm 0.33	53.02 \pm 2.57	58.10 \pm 0.72	59.23 \pm 0.18
FIARSE	78.78 \pm 0.24	79.18 \pm 0.44	74.90 \pm 0.31	66.17 \pm 0.52	61.36 \pm 0.96	59.90 \pm 0.64	79.61 \pm 3.11	78.35 \pm 0.16	80.38 \pm 0.35	60.76 \pm 0.54	61.77 \pm 0.40	62.03 \pm 0.16
FedPPN	78.42 \pm 0.14	78.46 \pm 0.50	74.62 \pm 0.28	66.55 \pm 0.64	60.81 \pm 0.93	59.66 \pm 0.62	83.43 \pm 0.51	78.48 \pm 0.27	80.11 \pm 0.49	60.50 \pm 0.20	61.86 \pm 0.24	61.77 \pm 0.27
TRUST	78.73 \pm 0.32	78.14 \pm 0.18	74.04 \pm 0.31	65.15 \pm 0.52	63.51 \pm 0.31	60.43 \pm 0.27	84.94 \pm 0.27	83.25 \pm 0.28	82.14 \pm 0.13	62.34 \pm 0.24	65.12 \pm 0.27	65.34 \pm 0.45
FedGKC	82.35 \pm 0.32	81.25 \pm 0.51	77.29 \pm 0.34	68.79 \pm 0.37	67.27 \pm 0.74	63.45 \pm 0.43	87.35 \pm 0.23	86.94 \pm 0.36	84.61 \pm 0.31	64.25 \pm 0.32	67.65 \pm 0.88	68.09 \pm 1.04

Method	CS			Physics			Photo			Computer		
	5	10	20	5	10	20	5	10	20	5	10	20
LG-FedAvg	90.64 \pm 0.47	88.04 \pm 0.42	85.32 \pm 0.54	94.42 \pm 0.33	93.87 \pm 0.39	93.45 \pm 0.28	89.96 \pm 0.52	87.91 \pm 0.44	85.59 \pm 0.49	85.77 \pm 0.41	85.53 \pm 0.46	84.76 \pm 0.50
FedProto	83.95 \pm 0.28	83.08 \pm 0.08	81.80 \pm 0.38	93.12 \pm 0.15	92.42 \pm 0.13	91.86 \pm 0.08	71.35 \pm 3.39	73.48 \pm 2.00	80.17 \pm 0.57	73.38 \pm 0.48	70.88 \pm 1.73	73.44 \pm 0.79
FML	89.23 \pm 0.46	86.65 \pm 0.42	85.76 \pm 0.51	94.60 \pm 0.29	93.91 \pm 0.36	92.11 \pm 0.33	82.65 \pm 0.44	87.68 \pm 0.47	85.50 \pm 0.39	86.19 \pm 0.48	85.28 \pm 0.40	84.60 \pm 0.45
FedKD	89.48 \pm 0.14	87.03 \pm 0.14	85.88 \pm 0.11	94.51 \pm 0.33	94.00 \pm 0.23	92.76 \pm 0.08	84.66 \pm 0.42	85.70 \pm 0.63	86.01 \pm 0.61	77.84 \pm 3.61	80.35 \pm 2.23	81.90 \pm 1.08
FedTGP	86.84 \pm 0.41	85.49 \pm 0.28	83.81 \pm 0.11	93.92 \pm 0.15	92.57 \pm 0.05	93.03 \pm 0.07	71.42 \pm 3.05	73.72 \pm 1.67	81.81 \pm 0.61	66.73 \pm 3.67	67.63 \pm 0.53	70.27 \pm 1.28
FIARSE	87.77 \pm 0.33	85.80 \pm 0.13	85.94 \pm 0.17	93.40 \pm 0.09	93.69 \pm 0.06	92.28 \pm 0.14	90.19 \pm 0.35	89.34 \pm 0.16	86.50 \pm 0.50	86.85 \pm 0.42	85.02 \pm 0.26	83.73 \pm 0.35
FedPPN	87.74 \pm 0.29	85.29 \pm 0.26	85.31 \pm 0.30	93.38 \pm 0.21	93.57 \pm 0.08	92.14 \pm 0.08	90.52 \pm 0.29	89.30 \pm 0.15	86.47 \pm 0.47	86.19 \pm 0.47	84.51 \pm 1.11	83.53 \pm 0.16
TRUST	88.94 \pm 0.26	87.35 \pm 0.24	84.54 \pm 0.26	94.23 \pm 0.51	93.35 \pm 0.37	92.21 \pm 0.25	88.51 \pm 0.34	87.81 \pm 0.43	85.85 \pm 0.16	85.84 \pm 0.28	84.63 \pm 0.26	83.76 \pm 0.42
FedGKC	92.58 \pm 0.42	90.91 \pm 0.18	88.50 \pm 0.15	95.35 \pm 0.23	94.78 \pm 0.15	93.84 \pm 0.15	92.87 \pm 0.28	90.54 \pm 0.31	89.86 \pm 0.36	89.54 \pm 0.31	87.64 \pm 0.40	86.48 \pm 0.32

architectures. We utilize five distinct two-layer graph neural network architectures: GCN [15], GAT [32], GraphSAGE [7], GIN [39], and SGC [35]. (2) **Varying model scales.** We leverage deep GNNs technology [40] to employ a lightweight two-layer SGC, a conventional two-layer GCN, and deeper models including four-layer GCN, six-layer GCN, and eight-layer GCN. For the allocation of clients, given K clients, the model architecture assigned to the k -th client is determined by $(k \bmod 5)$, $k \in [K]$. The parameters of each assigned model architecture are re-initialized for every client.

5.2 Performance Comparison

To answer Q1, we conduct comprehensive experiments under heterogeneous and non-heterogeneous settings. Overall, FedGKC exhibits consistent improvements over all selected MHTFL baselines.

Table 3: Comparison of our method with other federated methods with 10 clients in non-heterogeneous settings.

	CS	Physics	Photo	Computer	Avg.
FedAvg	81.06 \pm 0.62	92.71 \pm 0.47	78.02 \pm 0.53	66.90 \pm 0.71	79.67 \pm 0.58
MOON	85.02 \pm 0.44	94.37 \pm 0.68	80.37 \pm 0.59	69.50 \pm 0.41	82.32 \pm 0.52
FedDC	83.71 \pm 0.71	93.04 \pm 0.55	72.99 \pm 0.66	63.35 \pm 0.79	78.27 \pm 0.63
FedSage+	84.83 \pm 0.39	92.96 \pm 0.48	79.21		

Table 4: The experimental results by incorporating the proposed key components into the baseline. "SMKD" indicates Self-Mutual Knowledge Distillation, and "KAMA" indicates Knowledge-Aware Model Aggregation.

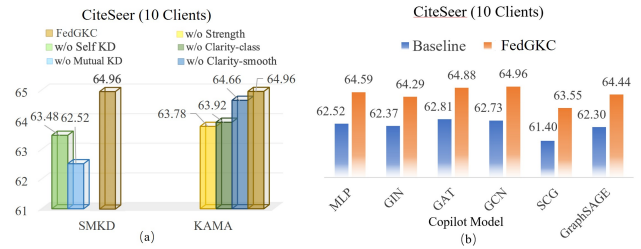
		Cora				CiteSeer				PubMed			
SMKD	KAMA	Client 5	Client 10	Client 20	Avg.	Client 5	Client 10	Client 20	Avg.	Client 5	Client 10	Client 20	Avg.
		80.50 \pm 0.41	79.54 \pm 0.36	75.21 \pm 0.58	78.42 \pm 0.45	64.74 \pm 0.47	62.73 \pm 0.39	60.90 \pm 0.55	62.82 \pm 0.47	84.64 \pm 0.33	83.15 \pm 0.28	81.87 \pm 0.42	83.22 \pm 0.34
✓		81.41 \pm 0.45	80.44 \pm 0.37	74.50 \pm 0.52	78.79 \pm 0.45	64.44 \pm 0.46	64.29 \pm 0.44	60.88 \pm 0.49	63.20 \pm 0.46	84.54 \pm 0.41	83.37 \pm 0.35	82.51 \pm 0.40	83.47 \pm 0.39
	✓	81.24 \pm 0.39	79.73 \pm 0.41	75.03 \pm 0.46	78.67 \pm 0.42	65.04 \pm 0.42	63.11 \pm 0.38	61.03 \pm 0.51	63.06 \pm 0.44	85.05 \pm 0.36	83.20 \pm 0.33	82.27 \pm 0.40	83.51 \pm 0.36
✓	✓	81.42 \pm 0.45	80.71 \pm 0.62	75.38 \pm 0.38	79.17 \pm 0.48	67.19 \pm 0.46	65.15 \pm 0.73	61.40 \pm 0.67	64.58 \pm 0.62	85.54 \pm 0.16	83.48 \pm 0.25	82.42 \pm 0.11	83.81 \pm 0.17

datasets and client configs, surpassing KD and prototype-based methods. Two strong partial-model strategies (i.e., FIARSE, FedPPN) exhibit competitive results due to their effective submodel selection and parameter coverage. However, their performances are less stable when architectural heterogeneity increases, as partial extraction/mapping struggles to preserve topology-aware signals across diverse GNN designs. In contrast, FedGKC decouples cross-client exchange via copilot models and integrates topology-aware distillation, resulting in superior overall accuracy and more robust transfer. **(2) Clients with Different Model Scales.** In the second scenario, we consider the variations in model scales due to differences in the computational capabilities of various client devices. As shown in Table 2, FedGKC demonstrates superior performance on the test set compared to other methods, with an average of 4.40% higher accuracy than FML and 4.22% higher accuracy than FedKD. It confirms that FedGKC can not only adapt to the heterogeneity of simple model architectures, but can also be extended to models of different scales, and performs well. **(3) Comparative Experiments under Non-Heterogeneous Settings.** In addition to the experiments under heterogeneous settings, we also conduct comparative experiments in non-heterogeneous settings to evaluate the performance of FedGKC in traditional federated learning environments. The results in Table 3 show that despite being specifically designed for heterogeneous client scenarios, FedGKC performs exceptionally well even in non-heterogeneous settings, outperforming the baseline approach FedAvg by 10.5% on average. FedGKC even surpasses federated learning methods tailored for homogeneous clients by an average of 1.07% over the suboptimal method Fed-Pub, which further validates the generality and robustness of FedGKC.

5.3 Ablation Study

To address Q2, we perform ablation experiments on the two key modules of FedGKC: Self-Mutual Knowledge Distillation (SMKD) and Knowledge-Aware Model Aggregation (KAMA). Table 4 reports the results when each module is applied independently. Specifically, when SMKD is used alone, the server employs a sample-size-based aggregation strategy; when KAMA is used alone, clients adhere to a conventional dual-model architecture. The results show that SMKD provides notable improvements on Cora and CiteSeer, while KAMA contributes more strongly on PubMed, suggesting that KAMA is particularly advantageous for larger-scale datasets. Combining both modules yields the best overall performance across all benchmarks.

To further disentangle the contributions of individual mechanisms, we conduct a fine-grained ablation on the CiteSeer with 10 clients, as shown in Fig. 3(a). For the SMKD module, we separately remove the self-distillation and mutual distillation components. Results indicate that eliminating self-distillation weakens the model's

**Figure 3: (a) Ablation experiments of SMKD and KAMA. (b) Coarse local-copilot Alignment vs. full FedGKC using different model Architectures on the copilot model.**

ability to optimize its own representations, while removing mutual distillation forces clients to rely solely on local data, thereby hindering global knowledge assimilation and degrading overall performance. For the KAMA, we ablate the three factors forming knowledge weights: knowledge strength, class-level knowledge clarity (the first term in Eq. (7)), and association clarity (the second term in Eq. (7)). We find that knowledge strength plays the most decisive role in aggregation, whereas the others exert relatively smaller but positive effects, enhancing both stability and accuracy.

5.4 Generalization and Sensitivity Analysis

To answer Q3, we investigate the effectiveness of mutual distillation module when deploying varying architectures on copilot model in Fig. 3(b). Baseline refers to removal of carefully designed loss objectives and KAMA-related mechanism while applying various model architectures on copilot model. As results demonstrate, full FedGKC demonstrates significant performance improvements across choices of most widely adopted model architectures, further validating the flexibility and generalizability of FedGKC's design.

To answer Q4, we evaluate the performance of FedGKC using 20 clients from the CS dataset across various hyperparameter settings. Specifically, we explore various combinations of the trade-off parameters α and β in Eq. (2) and Eq. (3). The results in Fig. 4(a) indicate that FedGKC performs optimally with α set between 0.6 and 0.7, and β maintained within the range of 0.1 to 0.2. Accordingly, we finalize our hyperparameters with $\alpha = 0.6$ and $\beta = 0.2$. Additionally, we conduct a sensitivity analysis on λ in Eq. (7), which represents the influence of over-smoothing on the clarity of node knowledge. From Fig. 4(b), we find that setting λ to 0.1 effectively enhances model performance, whereas excessively high values lead to performance deterioration. It underscores the importance of balancing node similarity and the over-smoothing issue.

6 Conclusion

This paper introduces FedGKC, a knowledge-driven FGL framework resolving the model-heterogeneity challenge. By coupling

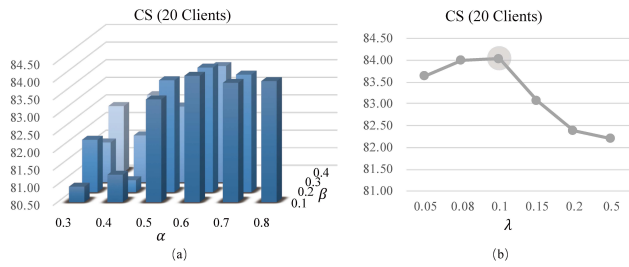


Figure 4: Hyperparameters analysis: (a) Different combinations between parameters α and β . (b) Different λ values.

mutual knowledge distillation between each local model and globally trained copilot model and performing knowledge-aware aggregation on the server, FedGKC enables clients with different model architectures to collaborate without sharing raw data. Empirically and theoretically, FedGKC demonstrates robust performance and stable optimization while keeping communication efficient. Future works include improving knowledge transfer on graphs, and refining mechanisms to further balance efficiency and accuracy.

References

- [1] Samiul Alam, Luyang Liu, Ming Yan, and Mi Zhang. 2022. Fedrolex: Model-heterogeneous federated learning with rolling sub-model extraction. *Advances in neural information processing systems* 35 (2022), 29677–29690.
- [2] Jinheon Baek, Wonyong Jeong, Jiongdao Jin, Jaehong Yoon, and Sung Ju Hwang. 2023. Personalized subgraph federated learning. In *International conference on machine learning*. PMLR, 1396–1415.
- [3] Vincent D Blondel, Jean-Loup Guillaume, Renaud Lambiotte, and Etienne Lefevre. 2008. Fast unfolding of communities in large networks. *Journal of Statistical Mechanics: Theory and Experiment* 2008, 10 (oct 2008), P10008. <https://doi.org/10.1088/1742-5468/2008/10/P10008>
- [4] Xiwen Fang and Mang Ye. 2024. Noise-robust federated learning with model heterogeneous clients. *IEEE Transactions on Mobile Computing* (2024).
- [5] Kaituo Feng, Changsheng Li, Ye Yuan, and Guoren Wang. 2022. Freekd: Free-direction knowledge distillation for graph neural networks. In *Proceedings of the ACM SIGKDD Conference on Knowledge Discovery and Data Mining, KDD*.
- [6] Jiongyu Guo, Defang Chen, and Can Wang. 2022. Alignahead: online cross-layer knowledge extraction on graph neural networks. In *2022 International Joint Conference on Neural Networks (IJCNN)*. IEEE, 1–8.
- [7] Will Hamilton, Zhitao Ying, and Jure Leskovec. 2017. Inductive representation learning on large graphs. *Advances in neural information processing systems* 30 (2017).
- [8] Huarui He, Jie Wang, Zhanqiu Zhang, and Feng Wu. 2022. Compressing deep graph neural networks via adversarial knowledge distillation. In *Proceedings of the 28th ACM SIGKDD conference on knowledge discovery and data mining*. 534–544.
- [9] Xiangnan He, Kuan Deng, Xiang Wang, Yan Li, Yongdong Zhang, and Meng Wang. 2020. Lightgcn: Simplifying and powering graph convolution network for recommendation. In *Proceedings of the 43rd International ACM SIGIR conference on research and development in Information Retrieval*. 639–648.
- [10] Geoffrey Hinton. 2015. Distilling the Knowledge in a Neural Network. *arXiv preprint arXiv:1503.02531* (2015).
- [11] Weihua Hu, Matthias Fey, Marinka Zitnik, Yuxiao Dong, Hongyu Ren, Bowen Liu, Michele Catasta, and Jure Leskovec. 2020. Open graph benchmark: Datasets for machine learning on graphs. *Advances in neural information processing systems* 33 (2020), 22118–22133.
- [12] Wenke Huang, Guan Cheng Wan, Mang Ye, and Bo Du. 2023. Federated Graph Semantic and Structural Learning. In *Proceedings of the Thirty-Second International Joint Conference on Artificial Intelligence, IJCAI-23*, Edith Elkind (Ed.). International Joint Conferences on Artificial Intelligence Organization, 3830–3838. <https://doi.org/10.24963/ijcai.2023/426> Main Track.
- [13] Cuiying Huo, Di Jin, Yawen Li, Dongxiao He, Yu-Bin Yang, and Lingfei Wu. 2023. T2-gnn: Graph neural networks for graphs with incomplete features and structure via teacher-student distillation. In *Proceedings of the AAAI Conference on Artificial Intelligence*, Vol. 37. 4339–4346.
- [14] Houye Ji, Junxiong Zhu, Chuan Shi, Xiao Wang, Bai Wang, Chaoyu Zhang, Zixuan Zhu, Feng Zhang, and Yanghua Li. 2021. Large-scale Comb-K Recommendation. In *Proceedings of the Web Conference 2021 (Ljubljana, Slovenia) (WWW '21)*. Association for Computing Machinery, New York, NY, USA, 2512–2523. <https://doi.org/10.1145/3442381.3449924>
- [15] Thomas N Kipf and Max Welling. 2017. Semi-Supervised Classification with Graph Convolutional Networks. In *International Conference on Learning Representations*.
- [16] Sanjay Kumar, Abhishek Mallik, Anavi Khetarpal, and Bhawani Sankar Panda. 2022. Influence maximization in social networks using graph embedding and graph neural network. *Information Sciences* 607 (2022), 1617–1636.
- [17] Xunkai Li, Zhengyu Wu, Wentao Zhang, Yinlin Zhu, Rong-Hua Li, and Guoren Wang. 2023. FedGTA: Topology-Aware Averaging for Federated Graph Learning. *Proceedings of the VLDB Endowment* 17, 1 (2023), 41–50.
- [18] Zexi Li, Xinyi Shang, Rui He, Tao Lin, and Chao Wu. 2023. No fear of classifier biases: Neural collapse inspired federated learning with synthetic and fixed classifier. In *Proceedings of the IEEE/CVF International Conference on Computer Vision*. 5319–5329.
- [19] Paul Pu Liang, Terrance Liu, Liu Ziyin, Nicholas B Allen, Randy P Auerbach, David Brent, Ruslan Salakhutdinov, and Louis-Philippe Morency. 2020. Think locally, act globally: Federated learning with local and global representations. *arXiv preprint arXiv:2001.01523* (2020).
- [20] Tao Lin, Lingjing Kong, Sebastian U Stich, and Martin Jaggi. 2020. Ensemble distillation for robust model fusion in federated learning. *Advances in Neural Information Processing Systems* 33 (2020), 2351–2363.
- [21] Rui Liu, Pengwei Xing, Zichao Deng, Anran Li, Cuntai Guan, and Han Yu. 2024. Federated graph neural networks: Overview, techniques, and challenges. *IEEE Transactions on Neural Networks and Learning Systems* (2024).
- [22] Zhi Liu, Hanlin Zhou, Xiaohua He, Haopeng Yuan, Jiaxin Du, Mengmeng Wang, Guojiang Shen, Feng Xia, et al. 2024. Model-Heterogeneous Federated Graph Learning with Prototype Propagation. *IEEE Transactions on Artificial Intelligence* (2024).
- [23] Guodong Long, Yue Tan, Jing Jiang, and Chengqi Zhang. 2020. Federated learning for open banking. In *Federated learning: privacy and incentive*. Springer, 240–254.
- [24] Xiaofeng Lu, Yuying Liao, Chao Liu, Pietro Lio, and Pan Hui. 2021. Heterogeneous model fusion federated learning mechanism based on model mapping. *IEEE Internet of Things Journal* 9, 8 (2021), 6058–6068.
- [25] Julian McAuley, Christopher Targett, Qinfeng Shi, and Anton Van Den Hengel. 2015. Image-based recommendations on styles and substitutes. In *Proceedings of the 38th international ACM SIGIR conference on research and development in information retrieval*. 43–52.
- [26] Brendan McMahan, Eider Moore, Daniel Ramage, Seth Hampson, and Blaise Aguera y Arcas. 2017. Communication-efficient learning of deep networks from decentralized data. In *Artificial Intelligence and Statistics*. 1273–1282.
- [27] Oleksandr Shchur, Maximilian Mumme, Aleksandar Bojchevski, and Stephan Günnemann. 2018. Pitfalls of graph neural network evaluation. *arXiv preprint arXiv:1811.05868* (2018).
- [28] Tao Shen, Jie Zhang, Xinkang Jia, Fengda Zhang, Zheqi Lv, Kun Kuang, Chao Wu, and Fei Wu. 2023. Federated mutual learning: a collaborative machine learning method for heterogeneous data, models, and objectives. *Frontiers of Information Technology & Electronic Engineering* 24, 10 (2023), 1390–1402.
- [29] Yue Tan, Yixin Liu, Guodong Long, Jing Jiang, Qinghua Lu, and Chengqi Zhang. 2023. Federated learning on non-iid graphs via structural knowledge sharing. In *Proceedings of the AAAI Conference on Artificial Intelligence, AAAI*.
- [30] Yue Tan, Guodong Long, Lu Liu, Tianyi Zhou, Qinghua Lu, Jing Jiang, and Chengqi Zhang. 2022. Fedproto: Federated prototype learning across heterogeneous clients. In *Proceedings of the AAAI Conference on Artificial Intelligence*, Vol. 36. 8432–8440.
- [31] Yue Tan, Guodong Long, Jie Ma, Lu Liu, Tianyi Zhou, and Jing Jiang. 2022. Federated learning from pre-trained models: A contrastive learning approach. *Advances in neural information processing systems* 35 (2022), 19332–19344.
- [32] Petar Veličković, Guillem Cucurull, Arantxa Casanova, Adriana Romero, Pietro Liò, and Yoshua Bengio. 2018. Graph Attention Networks. In *International Conference on Learning Representations*.
- [33] Kai Wang, Yu Liu, Qian Ma, and Qian Z Sheng. 2021. Mulde: Multi-teacher knowledge distillation for low-dimensional knowledge graph embeddings. In *Proceedings of the Web Conference 2021*. 1716–1726.
- [34] Chuhan Wu, Fangzhao Wu, Lingjuan Lyu, Yongfeng Huang, and Xing Xie. 2022. Communication-efficient federated learning via knowledge distillation. *Nature communications* 13, 1 (2022), 2022.
- [35] Felix Wu, Amauri Souza, Tianyi Zhang, Christopher Fifty, Tao Yu, and Kilian Weinberger. 2019. Simplifying graph convolutional networks. In *International Conference on Machine Learning, ICML*.
- [36] Feijie Wu, Xingchen Wang, Yaqing Wang, Tianci Liu, Lu Su, and Jing Gao. 2024. FIARSE: Model-heterogeneous federated learning via importance-aware sub-model extraction. *Advances in Neural Information Processing Systems* 37 (2024), 115615–115651.
- [37] Zonghan Wu, Shirui Pan, Fengwen Chen, Guodong Long, Chengqi Zhang, and S Yu Philip. 2020. A comprehensive survey on graph neural networks. *IEEE transactions on neural networks and learning systems* 32, 1 (2020), 4–24.
- [38] Han Xie, Jing Ma, Li Xiong, and Carl Yang. 2021. Federated graph classification over non-iid graphs. *Advances in neural information processing systems* 34 (2021), 18839–18852.
- [39] Keyulu Xu, Weihua Hu, Jure Leskovec, and Stefanie Jegelka. 2018. How Powerful are Graph Neural Networks?. In *International Conference on Learning Representations*.
- [40] Keyulu Xu, Chengtao Li, Yonglong Tian, Tomohiro Sonobe, Ken-ichi Kawarabayashi, and Stefanie Jegelka. 2018. Representation Learning on Graphs with Jumping Knowledge Networks. In *Proceedings of the 35th International Conference on Machine Learning (Proceedings of Machine Learning Research, Vol. 80)*, Jennifer Dy and Andreas Krause (Eds.). PMLR, 5453–5462.
- [41] Bencheng Yan, Chaokun Wang, Gaoyang Guo, and Yunkai Lou. 2020. Tinygnn: Learning efficient graph neural networks. In *Proceedings of the 26th ACM SIGKDD International Conference on Knowledge Discovery & Data Mining*. 1848–1856.
- [42] Baoyao Yang, Pong C Yuen, Yiqun Zhang, and An Zeng. 2023. Allosteric feature collaboration for model-heterogeneous federated learning. *IEEE Transactions on Neural Networks and Learning Systems* (2023).
- [43] Cheng Yang, Jiawei Liu, and Chuan Shi. 2021. Extract the knowledge of graph neural networks and go beyond it: An effective knowledge distillation framework. In *Proceedings of the web conference 2021*. 1227–1237.
- [44] Yiding Yang, Jiayan Qiu, Mingli Song, Dacheng Tao, and Xinchao Wang. 2020. Distilling knowledge from graph convolutional networks. In *Proceedings of the IEEE/CVF conference on computer vision and pattern recognition*. 7074–7083.
- [45] Zhilin Yang, William Cohen, and Ruslan Salakhutdinov. 2016. Revisiting semi-supervised learning with graph embeddings. In *International conference on machine learning*. PMLR, 40–48.
- [46] Liping Yi, Gang Wang, Xiaoguang Liu, Zhuan Shi, and Han Yu. 2023. FedGH: Heterogeneous federated learning with generalized global header. In *Proceedings of the 31st ACM International Conference on Multimedia*. 8686–8696.

- [47] Liping Yi, Han Yu, Zhuan Shi, Gang Wang, Xiaoguang Liu, Lizhen Cui, and Xiaoxiao Li. 2023. FedSSA: Semantic similarity-based aggregation for efficient model-heterogeneous personalized federated learning. *arXiv preprint arXiv:2312.09006* (2023).
- [48] Rex Ying, Ruining He, Kaifeng Chen, Pong Eksombatchai, William L. Hamilton, and Jure Leskovec. 2018. Graph Convolutional Neural Networks for Web-Scale Recommender Systems. In *Proceedings of the 24th ACM SIGKDD International Conference on Knowledge Discovery & Data Mining* (London, United Kingdom) (KDD '18). Association for Computing Machinery, New York, NY, USA, 974–983. <https://doi.org/10.1145/3219819.3219890>
- [49] Lu Yu, Shichao Pei, Lizhong Ding, Jun Zhou, Longfei Li, Chuxu Zhang, and Xiangliang Zhang. 2022. Sail: Self-augmented graph contrastive learning. In *Proceedings of the AAAI Conference on Artificial Intelligence*, Vol. 36. 8927–8935.
- [50] Jie Zhang, Song Guo, Xiaosong Ma, Haozhao Wang, Wenchao Xu, and Feijie Wu. 2021. Parameterized knowledge transfer for personalized federated learning. *Advances in Neural Information Processing Systems* 34 (2021), 10092–10104.
- [51] Jianqing Zhang, Yang Liu, Yang Hua, and Jian Cao. 2024. Fedtgp: Trainable global prototypes with adaptive-margin-enhanced contrastive learning for data and model heterogeneity in federated learning. In *Proceedings of the AAAI Conference on Artificial Intelligence*, Vol. 38. 16768–16776.
- [52] Ke Zhang, Carl Yang, Xiaoxiao Li, Lichao Sun, and Siu Ming Yiu. 2021. Sub-graph federated learning with missing neighbor generation. *Advances in Neural Information Processing Systems, NeurIPS* (2021).
- [53] Wentao Zhang, Xupeng Miao, Yingxia Shao, Jiawei Jiang, Lei Chen, Olivier Ruas, and Bin Cui. 2020. Reliable data distillation on graph convolutional network. In *Proceedings of the ACM on Management of Data, SIGMOD*.
- [54] Xiongtao Zhang, Ji Wang, Weidong Bao, Yaohong Zhang, Xiaomin Zhu, Hao Peng, and Xiang Zhao. 2024. Improving generalization and personalization in model-heterogeneous federated learning. *IEEE Transactions on Neural Networks and Learning Systems* (2024).
- [55] Xiao-Meng Zhang, Li Liang, Lin Liu, and Ming-Jing Tang. 2021. Graph neural networks and their current applications in bioinformatics. *Frontiers in genetics* 12 (2021), 690049.
- [56] Tong Zhao, Wei Jin, Yozen Liu, Yingheng Wang, Gang Liu, Stephan Günnemann, Neil Shah, and Meng Jiang. 2022. Graph data augmentation for graph machine learning: A survey. *arXiv preprint arXiv:2202.08871* (2022).
- [57] Zhuangdi Zhu, Junyuan Hong, and Jiayu Zhou. 2021. Data-free knowledge distillation for heterogeneous federated learning. In *International Conference on Machine Learning, ICML*. PMLR.

Table 5: Algorithm complexity analysis for existing prevalent FL and FGL studies.

Method	Client Memory	Server Memory	Inference Memory	Client Time	Server Time	Inference Time
FedAvg	$\mathcal{O}((b+k)f + f^2)$	$\mathcal{O}(Nf^2)$	$\mathcal{O}((b+k)f + f^2)$	$\mathcal{O}(kmf + nf^2)$	$\mathcal{O}(N)$	$\mathcal{O}(kmf + nf^2)$
MOON	$\mathcal{O}((b+k)f + Qf^2)$	$\mathcal{O}(Nf^2)$	$\mathcal{O}((b+k)f + f^2)$	$\mathcal{O}(kmf + nf^2 + Qnf)$	$\mathcal{O}(N)$	$\mathcal{O}(kmf + nf^2)$
FedSage+	$\mathcal{O}(L((n+sg)f + f^2))$	$\mathcal{O}(L(Nf^2))$	$\mathcal{O}(L((b+k)f + Lf^2))$	$\mathcal{O}(L((m+sg)f + (n+sg)f^2))$	$\mathcal{O}(N)$	$\mathcal{O}(L((m+sg)f + (n+sg)f^2))$
FGSSL	$\mathcal{O}(Q((b+k)f + f^2))$	$\mathcal{O}(Nf^2)$	$\mathcal{O}(L((b+k)f + Lf^2))$	$\mathcal{O}(Qkmf + Qnf^2)$	$\mathcal{O}(N)$	$\mathcal{O}(kmf + nf^2)$
Fed-PUB	$\mathcal{O}(M((b+k)f + f^2) + M^2)$	$\mathcal{O}(N(f^2 + M) + P_g)$	$\mathcal{O}(M((b+k)f + Mf^2))$	$\mathcal{O}(Mkmf + Mn f^2)$	$\mathcal{O}(N^2(\log(N) + M^2))$	$\mathcal{O}(Mkmf + Mn f^2)$
FedGTA	$\mathcal{O}((b+k)f + f^2 + kKc)$	$\mathcal{O}(Nf^2 + NkKc)$	$\mathcal{O}((b+k)f + f^2)$	$\mathcal{O}(km(f + knc) + n(f^2 + c))$	$\mathcal{O}(N + NkKc)$	$\mathcal{O}(kmf + nf^2)$
AdaFGL	$\mathcal{O}(E((b+k)f + f^2))$	$\mathcal{O}(Nf^2)$	$\mathcal{O}(E((b+k)f + f^2))$	$\mathcal{O}(E(kmf + nf^2))$	$\mathcal{O}(N)$	$\mathcal{O}(E(kmf + nf^2))$
FedGKC	$\mathcal{O}(2(b+l)f + 2f^2)$	$\mathcal{O}(Nf^2)$	$\mathcal{O}(2(b+l)f + 2f^2)$	$\mathcal{O}(kmf + nf^2 + f^2)$	$\mathcal{O}(N)$	$\mathcal{O}(kmf + nf^2)$

Outline

To meet page limits, we have included as much essential material as possible in the main text. The appendix provides supplementary details that complete our study. It is organized as follows:

- A Algorithm Complexity Analysis of existing FGL studies.
- B The Proof of Theorem Analysis presented in Sec. 4.
- C Detailed Implementations of Experiment.

A Algorithm Complexity Analysis

Table 5 summarizes the time and space complexity of different methods. Here, n , m , c , and f denote the numbers of nodes, edges, classes, and feature dimensions, respectively. s refers to the number of selected perturbed nodes, and g indicates the number of generated neighbors. b is the batch size. Parameters k and K represent the number of feature aggregation steps and the order of moments, respectively. N denotes the number of participating clients per round. Q corresponds to the query set size used in contrastive learning. E stands for the number of models in ensemble learning, M is the dimension of the trainable matrix for masking weights. P_g denotes the size of the pseudo-graph stored on the server.

Local updates play a key role in federated training efficiency. For example, for MOON and FGSSL, the cost of contrastive learning depends on the size and semantics of the query set, resulting in complexities of $\mathcal{O}(Qf^2)$ and $\mathcal{O}(Q((b+k)f + f^2))$, respectively, which may become prohibitive as local data grows. Ensemble-based AdaFGL maintains multiple local models to capture private semantics, bounded by $\mathcal{O}(E((b+k)f + f^2))$. Some approaches rely on additional message exchange. Specifically, FedSage+ requires client-to-client message sharing for subgraph augmentation, with complexity $\mathcal{O}(L((n+sg)f + f^2))$. Fed-PUB maintains a global pseudo-graph on the server and leverages uploaded weights for personalization, introducing a complexity of $\mathcal{O}(N(f^2 + M) + P_g)$. In contrast, FedGTA is relatively lightweight, using topology-aware soft labels for personalized aggregation on the server, but the extra encoding signal still incurs a complexity of $\mathcal{O}(kKc)$.

Compared with the above methods, our FedGKC demonstrates superior scalability in both time and space complexity. Its overall cost can be approximated as $\mathcal{O}(N((b+l)f + f^2))$, which grows linearly with the number of clients and standard graph operations, without relying on large query sets, global pseudo-graphs, or multiple locally stored models. Moreover, FedGKC leverages lightweight self- and mutual-distillation for cross-model knowledge alignment on clients, and adopts a knowledge-aware aggregation scheme on the server, thereby avoiding heavy communication or redundant parameter updates. This enables FedGKC to maintain low computational and storage overhead while significantly improving accuracy,

striking a favorable balance between efficiency and performance, which highlight FedGKC’s advantage over existing baselines.

B The Proof of Theoretical Analysis

In this section, we present comprehensive derivations and rigorous proofs for Theorem 2 and Theorem 3.

B.1 The Proof of Theorem 2

This theorem establishes the relationship between the node score S_i and its underlying components of knowledge strength and knowledge clarity, thereby characterizing how the scoring mechanism reflects both confidence and smoothness.

Proof. Because $\sum_c p_{i,c} = 1$ and $\sum_{c \neq \arg \max p_i} p_{i,c} = 1 - m_i$, we can reformulate the definition of knowledge intensity into the following mathematical expression:

$$Q_i^{\text{clar}} = \frac{1}{M-1} (m_i - (1 - m_i)) - \lambda \overline{\text{sim}}_i = \frac{2m_i - 1}{M-1} - \lambda \overline{\text{sim}}_i. \quad (17)$$

Accordingly, the node score S_i is formulated as the aggregation of knowledge strength and knowledge clarity, which can be expressed as Eq. (14). Subsequently, we compute the partial derivatives of m_i and $\overline{\text{sim}}_i$ in Eq. (14), which leads to the following result:

$$\frac{\partial S_i}{\partial m_i} = \alpha = 1 + \frac{2}{M-1}, \quad \frac{\partial S_i}{\partial \overline{\text{sim}}_i} = -\lambda. \quad (18)$$

The first partial derivative is strictly positive, whereas the second partial derivative is strictly negative.

In summary, this proof shows that the proposed aggregation weights assign higher scores to nodes with greater confidence, while simultaneously penalizing excessive oversmoothing. This property ensures that the scoring mechanism captures meaningful knowledge quality in a theoretically consistent manner.

B.2 The Proof of Theorem 3

This theorem formally characterizes the discrepancy between the alignment of KAMA and FedAvg, and proves that the gradient direction induced by KAMA approaches the global optimal gradient direction more closely.

Proof. According to the definition of the knowledge-related weight, we obtain:

$$\sum_k w_k^{\text{know}} a_k = \frac{\sum_k P_k a_k}{\sum_j P_j} = \frac{K(\bar{P} \bar{a} + \text{Cov}(P, a))}{K \bar{P}} = \bar{a} + \frac{\text{Cov}(P, a)}{\bar{P}}. \quad (19)$$

Initially, we need to unify the numerator and denominator.

$$\sum_k w_k^{\text{know}} a_k = \frac{\sum_k P_k a_k}{\sum_j P_j} = \frac{\sum_k P_k a_k}{K \bar{P}}. \quad (20)$$

Table 6: Statistics of the eight employed benchmark datasets.

Dataset	Nodes	Features	Edges	Classes	Train/Val/Test
Cora	2,708	1,433	5,429	7	20%/40%/40%
CiteSeer	3,327	3,703	4,732	6	20%/40%/40%
PubMed	19,717	500	44,338	3	20%/40%/40%
CS	18,333	6,805	81,894	15	20%/40%/40%
Physics	34,493	8,415	247,692	5	20%/40%/40%
Photo	7,487	745	119,043	8	20%/40%/40%
Computer	13,381	767	245,778	10	20%/40%/40%
ogbn-arxiv	169,343	128	2,315,598	40	60%/20%/20%

Next, we decompose the numerator by writing $P_k = (P_k - \bar{P}) + \bar{P}$:

$$\begin{aligned}
\sum_k P_k a_k &= \sum_k \left((P_k - \bar{P}) + \bar{P} \right) a_k = \bar{P} \sum_k a_k + \sum_k (P_k - \bar{P}) a_k \\
&= K\bar{P}\bar{a} + \sum_k (P_k - \bar{P}) ((a_k - \bar{a}) + \bar{a}) \\
&= K\bar{P}\bar{a} + \underbrace{\sum_k (P_k - \bar{P}) (a_k - \bar{a})}_{K\text{Cov}(P, a)} + \underbrace{\bar{a} \sum_k (P_k - \bar{P})}_0 \\
&= K\bar{P}\bar{a} + K\text{Cov}(P, a).
\end{aligned} \tag{21}$$

Here we use $\sum_k (P_k - \bar{P}) = 0$ and the covariance definition:

$$\text{Cov}(P, a) := \frac{1}{K} \sum_{k=1}^K (P_k - \bar{P}) (a_k - \bar{a}). \tag{22}$$

Substituting this decomposition back into the previous expression, we obtain:

$$\sum_k w_k^{\text{know}} a_k = \frac{K(\bar{P}\bar{a} + \text{Cov}(P, a))}{K\bar{P}} = \bar{a} + \frac{\text{Cov}(P, a)}{\bar{P}}. \tag{23}$$

Finally, this leads to the formulation of KAMA, whose inner product can be expressed as:

$$\begin{aligned}
\langle \hat{g}_{\text{KAMA}}, g^* \rangle &= \sum_k \frac{1}{2} (w_k^{\text{vol}} + w_k^{\text{know}}) a_k \\
&= \frac{1}{2} \sum_k w_k^{\text{vol}} a_k + \frac{1}{2} \sum_k w_k^{\text{know}} a_k \\
&= \frac{1}{2} \underbrace{\langle \hat{g}_{\text{FedAvg}}, g^* \rangle}_{\sum_k w_k^{\text{vol}} a_k} + \frac{1}{2} \left(\bar{a} + \frac{\text{Cov}(P, a)}{\bar{P}} \right).
\end{aligned} \tag{24}$$

Consequently, Eq. (16) is established. This positive discrepancy confirms that the gradient descent direction under KAMA exhibits superior alignment with the global optimum compared to FedAvg.

C Detailed Implementation of Experiment

Table 6 display the statistical information of selected datasets for our experiment, which have been widely applied in Graph Machine Learning research. This section displays dataset descriptions and experimental environments.

C.1 Toy Experiment Implementation

The simulation settings and experimental environment is aligned with description in Sec. 5.1. Experiment is conducted on the Cora dataset, which is further partitioned into 10 clients. Representative baselines selected for each category are most competitive MHTFGL methods to our knowledge: FML [28] for Partial Model, FedPPN [22] for Prototype, and ALFeCo [42] for Public/Synthetic Information.

C.2 Dataset Descriptions

Cora, **CiteSeer**, and **PubMed** are three citation network datasets. Nodes represent papers and edges represent citation relationships. The node features are word vectors, where each element indicates the presence or absence of each word.

CS, **Physics** are co-authorship graphs derived from the MAG. In these graphs, nodes represent individual authors, edges denote co-authorship relationships between them, and node features are constructed from the keywords of the authors' publications. The labels assigned to the nodes indicate the specific research fields in which the authors are active. These datasets are commonly used for evaluating graph-based methods, particularly for node classification.

Photo and **Computers** are segments of the Amazon co-purchase graph, where nodes represent items and edges represent that two goods are frequently bought together. Given product reviews as bag-of-words node features.

ogbn-arxiv are two citation graphs indexed by MAG. Each paper involves averaging the embeddings of words in its title and abstract. The embeddings of individual words are computed by running the skip-gram model.

C.3 Implementation Details

The experiments are conducted on an NVIDIA GeForce RTX 3090 GPU. Unless otherwise specified, the copilot model employed is a two-layer GCN architecture. The evaluation metric focuses on node classification accuracy within subgraphs on the client side, with performance averaged across all clients. The Adam optimizer is selected for the optimization process. For hyperparameter values, α and β in Eq. (2) and Eq. (3) are set to 0.6 and 0.2, respectively, and λ in Eq. (7) is set to 0.1. The evaluation metric is the node classification accuracy on the test set. To ensure reproducibility, the complete code for implementing the FedGKC is released publicly at <https://anonymous.4open.science/r/FedGKC-65BD/>.